UDC 550.8+528.4
DOI: http://doi.org/10.17721/1728-2713.108.13

Vasyl HUDAK, PhD Student,
ORCID ID: 0009-0002-7333-0409
e-mail: gudak_vasyl@knu.ua
Taras Shevchenko National University of Kyiv, Kyiv, Ukraine

Tetiana KRIL, PhD (Geol.)
ORCID ID: 0000-0002-4324-9231
e-mail: kotkotmag@gmail.com
Institute of Geological Sciences, NAS of Ukraine, Kyiv, Ukraine

Vitaliy ZATSERKOVNYI, DSc (Techn.), Prof.
ORCID ID: 0009-0003-5187-6125
e-mail: vitalii.zatserkovnyi@knu.ua
Taras Shevchenko National University of Kyiv, Kyiv, Ukraine

REMOTE SENSING ANALYSIS OF VERTICAL SURFACE DISPLACEMENTS AS AN INDICATOR OF UNDERGROUND STRUCTURE DEFORMATIONS

(Представлено членом редакційної колегії д-ром геол. наук, проф. С.А. Вижвою)

Background. *The paper is devoted to the analysis of vertical displacements based on remote sensing data as an identifier of hazardous engineering-geological processes in areas with underground infrastructure. The study was carried out on the example of the section of the tunnel between Demiivska and Lybidska stations of the Kyiv subway. In December 2023, processes of uneven compaction and vibration creep of the soil massif around the tunnel lining were detected, and there was a risk of loss of stability of the tunnel structures and an emergency.*

Methods. *This study employs the Differential Interferometric Synthetic Aperture Radar (D-InSAR) method which allows monitoring of soil surface deformations through phase change analysis among radar images. The correction procedures were applied to mitigate noise in processed images caused by temporal and geometric decorrelation, atmospheric disturbances, and other noise interferences. Correction and filtering method, specifically Canny and Sobel linear filters, were used to improve accuracy. Their application to processed satellite images enhances the contours of recorded vertical displacements and reduces geometric distortion noise, preserving the structural integrity of the images. According to our calculations, effective anomaly detection in images of urbanized areas requires a minimum threshold of 25 % in image contrast and clarity. The filters' application for highlighting significant intensity changes achieved a 28 % increase in clarity, indicating high processing effectiveness for further analysis of displacement maps and other parameters related to vertical shifts.*

Results. *Abnormal zones of vertical displacements were identified within the study area based on vertical displacement data. During the 2022–2023 observation period, these zones shifted toward the metro tunnel axis. Vertical displacements directly above the area of subsidence near the 'Rozetka' store were detected during the fifth observation period, October–December 2023, coinciding with the tunnel closure for repairs. Overall, displacement values shifted from negative in 2022 to positive in 2023, suggesting that displacements may have served as an early indicator of underground structure deformation activation. The use of filters allowed for more precise identification of displacement dynamics and localization of deformation zones throughout the observation periods. In the final period, the anomalous zone aligned with the location of tunnel deformations and recorded surface subsidence.*

Conclusions. *Using the example of the distillation tunnel section, we demonstrate the possibility of using the analysis of vertical surface displacements performed by D-InSAR together with a combination of Kenny and Sobel filters to track vertical surface displacements, which is important for monitoring the condition of underground facilities and preventing possible accidents. This study lays the foundation for further development of methodological approaches to the analysis of potential deformations of underground structures based on surface dynamics (vertical displacements). Further improvement of the methodology will help to ensure the accuracy and reliability of data in the context of monitoring underground structures.*

Keywords: *Vertical surface displacements, satellite images, D-InSAR, underground structures, Demiivska metro accident.*

Background

The ability to predict the effects of hazardous geological processes on underground infrastructure, with the aim of preventing emergencies and avoiding economic and social repercussions, represents a critical challenge in assessing natural risks and disasters. Solving this issue involves two main approaches: the first approach includes targeted in-situ field research aimed at understanding the nature and refining the mechanisms behind hazardous phenomena within geological environments, taking into account natural factors and anthropogenic impacts; the second involves the development of modern, effective information and analytical tools to forecast and prevent the consequences of such processes, ensuring stable operation of engineering structures and safeguarding human life.

Large cities are often characterized by noncompliance with functional zoning standards (Ministry of Regional Development of Ukraine, 2018); for instance, energy facilities are sometimes placed unsystematically, occasionally located near residential areas, and roads with heavy traffic are often situated near residential neighborhoods. The close proximity of industrial, transport, and residential facilities, combined with complex engineering-geological conditions, can lead to increased intensity of anthropogenic impact, thereby triggering hazardous engineering-geological processes and, consequently, accidents and emergencies. Urban development impacts the geological environment in stages: from the destruction of natural surroundings (e.g., removal of vegetation and soil layers, excavation) to the introduction of new elements into the natural system (e.g., buildings, underground structures, paved areas). Ensuring the reliability and cost-effectiveness of shallow underground structures, which are characteristic of urban construction, is therefore essential for the investment attractiveness of developing underground urban infrastructure.

In early December 2023, train movement on the Obolonsko-Teremkivska line of the Kyiv Metro was suspended along the section of the running tunnel between Demiivska and Lybidska stations. This section was closed for repairs (Fig. 1b) due to the discovery of uneven soil loosening, vibrocreep processes around the tunnel, and additional loading on the tunnel lining, leading to a risk of tunnel structure instability (Kyiv City Council, 2023). Surface subsidence was also recorded near the 'Rozetka' store (Fig. 1a).

ISSN 1728-3817

a *b*

Fig. 1. Surface deformation (a) and repair work on the tunnel section (b)
(a – photo by Vlad Kolodiy/Suspilne Kyiv, 2023; b – photo by Telegraf, 2024)

This area is located at the intersection of various functional zones within the city–transport, industrial, residential, and others. The natural geological conditions of the area are complicated by anthropogenic impact. Environmental disruption in urban settings is often associated with the chaotic placement of structures from different functional zones. The most critical influences arise from changes in water levels and soil moisture. The effect of soil moisture is indirect, manifesting as increased pore pressure and higher soil humidity. Rising water levels lead to shifts in stress distribution within the subsurface, causing greater vertical displacement of soil particles (Kril, 2017). Increased soil moisture accelerates the propagation of longitudinal waves under dynamic loads, such as those generated by metro trains.

The construction of tunnels between Demiivska and Lybidska stations was carried out from 2004 to 2006. A significant portion of the tunnel lies in a floodplain and passes beneath the Lybid River. Under such challenging geological conditions, the tunnel was constructed using underground techniques with artificial water-level lowering. During metro construction and the reconstruction of the transportation interchange at Demiivska Square, cracks were observed in nearby buildings, including structural elements of the Vernadsky Library and facade damage (Kril, 2017).

The geological crosssection of this area, from top to bottom, comprises technogenic deposits (tH), alluvial soils (loams, sandy loams, sands) (aH), ravine deposits represented by sands and sandy loams (adP_{III}-H), loess-like sandy loams and loams ($edvP_{III}$-H), clay marls (₱$_2$kv), and sands of the Buchach series (₱$_2$bc). These varieties of loose soils are sensitive to subsidence and settling processes, particularly under conditions of increased moisture. Surface deformation studies, which serve as indirect markers of changes within the geotechnical environment of areas with such engineering-geological conditions, are justified and advisable to conduct using remote sensing methods.

The review of methods used in the investigation of failures in underground infrastructure (Minh et al., 2020; Italian National Research Council, 2017) highlights the significant potential of interferometric approaches for image processing. These methods support the monitoring and analysis of near-surface conditions, which are critical for ensuring safety and assessing damages. The primary methods include:

- Differential Interferometric Synthetic Aperture Radar (D-InSAR): D-InSAR identifies maximum deformation gradients, making it effective for monitoring rapid changes caused by underground activities. This method excels in urban areas where even minor displacements may have considerable implications for infrastructure. Unlike traditional InSAR, D-InSAR measures dynamic surface changes between two time points, allowing monitoring vertical or horizontal deformations caused by events such as earthquakes, volcanic eruptions, ground subsidence, or glacier movement (Serco Italia SPA, 2018).
- Small Baseline Subset (SBAS): SBAS provides lower-noise results, proving useful for safety pillar analysis in regions with hazardous engineering-geological processes. By processing data from multiple images, SBAS reduces noise, yielding more accurate insights into ground deformations (Pawluszek-Filipiak et al., 2022, Iglesias et al., 2015). This method is especially valuable for detecting long-term changes, focusing on small but stable displacements. However, it may be less effective at capturing extreme deformation gradients compared to methods like D-InSAR, which is critical in cases with sudden or localized deformations. Consequently, combining SBAS with other methods is important for a comprehensive analysis of deformation processes.
- Persistent Scatterer Interferometry (PS-InSAR): PS-InSAR is an advanced method that allows for high-resolution monitoring of vertical surface displacements (Ferretti, 2000; Nguyen et al., 2020). This technique relies on persistent scatterers – objects that remain stable over long periods and can be consistently identified in radar images. This method enables researchers to capture small displacements accurately, even under significant noise levels (Zhang et al., 2019). However, PS-InSAR also has limitations, such as dependency on a sufficient density of scatterers within the study area. In regions with low scatterer density, the method may not produce optimal results. Similar to SBAS, PS-InSAR provides reliable results in stable areas but is less sensitive to rapid changes than D-InSAR (Pawluszek-Filipiak et al., 2022).

Despite the valuable information that these methods can provide, there are issues such as geologic noise and signal strengths that can complicate the process of detecting vertical displacements. Geologic noise refers to natural variations and irregularities on the Earth's surface that can be caused by various factors such as landforms, vegetation, and seismic activity, which can interfere with the clarity of measurements (Caduff et al., 2015, Gabriel et al., 1989). This emphasizes the need for continuous improvement of processing procedures to increase their efficiency and accuracy in detecting subtle displacements.

The objective of the study is to quantify vertical surface displacements in areas with underground structures in order to evaluate surface dynamics as an indicator of the development of deformations. The following tasks were undertaken:

- Selection under specific conditions and collection of satellite data from March 2022 to December 2023;

• Processing of data using the D-InSAR method in the SNAP software environment;

• Reclassification of processed images through linear normalization of displacement scales;

• Detection of anomalous zones within the study area using linear filtering methods;

• Interpretation of results.

Methods

The D-InSAR method is an image processing technique based on Synthetic Aperture Radar (SAR) technology, allowing for the detection of Earth's surface deformations and changes by comparing radar images acquired at different times. D-InSAR utilizes existing SAR images, applying phase change analysis between images to detect even minor surface shifts with high precision. This method involves the analysis of paired images to identify surface changes between two points in time. From each pair, an interferogram is computed, providing information on surface displacements. For instance, a dataset of five images would generate sequential pairs. The method processes images based on their coherence but has limitations that can impact the accuracy of deformation measurements, reducing spatial and temporal coherence, which complicates the study of displacements (Kril, & Orlenko, 2022).

In this study, radar satellite images from the Sentinel-1A satellite, with a spatial resolution of 10 meters in paired mode, were selected to calculate vertical displacements of the Earth's surface between the Demiivska and Lybidska metro stations (see Tab. 1). The images covered the periods from March to October, October to December, and December to March 2022–2023, thus minimizing the influence of vegetation on the results. The images were downloaded in Single Look Complex (SLC) format from the official Alaska Satellite Facility (ASF Data Search, 2024) website. SAR images contain data as discrete integer Digital Number (DN) values, where each pixel's DN corresponds to the radar signal's reflectivity from a specific area of the Earth's surface (Serco Italia SPA, 2018). Processing was conducted using the open-source Sentinel Application Platform (SNAP).

Table 1

Description of analysis periods for selected Sentinel-1A paired radar images

№ of period	Duration of period	Details of paired radar images
1st	March – October 2022	S1A_IW_SLC__1SDV_20220315T154613_20220315T154646_042334_050BF4_828B S1A_IW_SLC__1SDV_20221029T154623_20221029T154656_045659_0575C5_5595
2nd	October – December 2022	S1A_IW_SLC__1SDV_20221005T154623_20221005T154653_045309_056AB6_F51F S1A_IW_SLC__1SDV_20221216T154621_20221216T154651_046359_058D81_DC17
3rd	December 2022 – March 2023	S1A_IW_SLC__1SDV_20221204T154622_20221204T154655_046184_05878D_ED29 S1A_IW_SLC__1SDV_20230322T154619_20230322T154651_047759_05BCC9_F365
4th	March– October 2023	S1A_IW_SLC__1SDV_20230310T154619_20230310T154651_047584_05B6DB_2DBD S1A_IW_SLC__1SDV_20231024T154628_20231024T154701_050909_0622FE_1382
5th	October– December 2023	S1A_IW_SLC__1SDV_20231012T154603_20231012T154630_050734_061D05_4CBE S1A_IW_SLC__1SDV_20231211T154627_20231211T154700_051609_063B2B_1AF4

Based on interferometric processing of radar data from the study area, surface deformation characteristics were obtained, specifically values for vertical displacements of the Earth's surface (Fig. 2).

As mentioned earlier, the accuracy of the results depends not only on the aforementioned factors but also on the reliability of information about the imaging system's parameters (Orlenko, 2024). The baseline, which defines the satellite configuration, has the greatest impact on accuracy, as even minor changes in the phase center can significantly affect the interferometric phase (Piestova et al., 2020). To improve result accuracy, it is necessary to consider these factors and apply corrective methods.

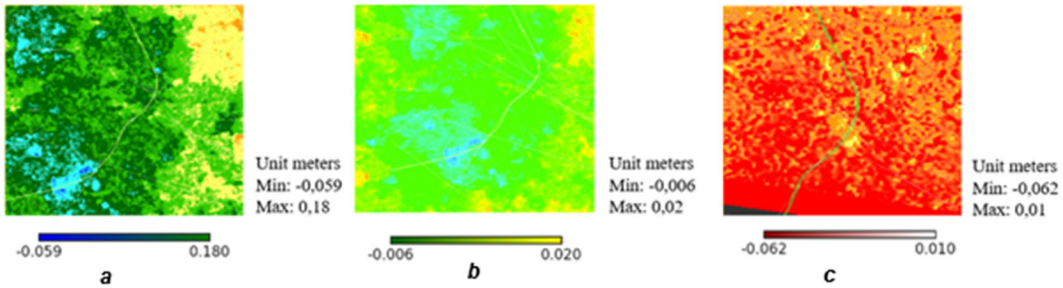

Fig. 2. Vertical displacement maps for the study area, generated using the D-InSAR method from Sentinel-1A image pairs:
a) – 1st period; b) – 2nd period; c) – 3rd period

However, the real images, along with useful information, contain various noise types (Orlenko, 2024; Serco Italia SPA, 2018), including coherence noise arising from signal decorrelation between two images, especially in urban areas with rapidly changing surfaces and multiple reflectors. Additionally, moving objects like vehicles and pedestrians can create local phase distortions that complicate measurement accuracy (geometric distortion noise). Shadowing and multipath noise is caused by multiple signal reflections from different surfaces (e.g., building walls), which is especially relevant in densely built-up areas. Topographic distortions, due to shadow and overlay effects from complex terrain and tall objects, also lead to errors in height and position determination. Atmospheric noise, caused by variations in atmospheric humidity and temperature profiles between imaging times, further affects measurement accuracy, which can be intensified in urban climates. In urban areas, radio frequency interference from local sources, such as antennas, radio, and TV transmitters, may also reduce interferometric data quality by introducing additional radar signal disturbances.

To mitigate these effects, local filtering is frequently applied in practice, where integration and averaging are conducted over a relatively small neighborhood around each image point, rather than across the entire determination area x and y. The point spread function in this case has limited dimensions. This approach provides the advantage of fast processing. When working with raster images consisting of individual pixels, integration is replaced by summation. The linear transformation in the case of local filtering takes the following form (Forsyth, & Ponce, 2012):

$$g_{ij} = \sum_D a_{kl} f_{i+kj+l}, \quad (1)$$

where *g* represents the linear transformation, summing over a neighborhood *D* of the point *(i, j)* and a_{kl} denotes the point spread function value in this neighborhood.

The pixel brightness *f* at point *(i, j)* and in its neighborhood is multiplied by coefficients a_{kl} and the transformed brightness of the *(i, j)*-th pixel is the sum of these products. Typically, the set a_{kl} is represented as a rectangular matrix (mask), for example, with a size of *3×3*.

The matrix elements satisfy the condition of spatial invariance. Filtering is performed by shifting the mask from left to right (or top to bottom) by one pixel (Sonka et al., 2014). At each position, the above operations are performed, specifically multiplying the weight factors a_{kl} with the corresponding brightness values of the original image and summing the products. The resulting value is assigned to the central *(i, j)*-th pixel.

The mask typically has an odd number of rows and columns to uniquely identify the central element. The described filtering procedure is characterized by the fact that the output filter values *g* depend solely on the input values *f*. Such filters are called non-recursive, while filters where the output values *g* depend not only on the input values *f* but also on previous output values are called recursive (Forsyth, & Ponce, 2012).

Linear filters can be used not only to reduce noise but also to enhance brightness gradients and highlight edges. Vertical gradients are detected by differentiating along rows, while horizontal gradients are detected along columns. Horizontal gradients can be identified by calculating the difference in pixel brightness along a row, equivalent to calculating the second derivative in the corresponding direction (Laplacian operator). Processed images (see Fig. 1) exhibit different maximum and minimum values and corresponding color scales, complicating further data interpretation. To standardize images and present results within a unified color range, reclassification was performed using linear normalization of the displacement scale. The displacement scale normalization methodology enables a more effective analysis and interpretation of changes in the data. The normalization formula is as follows:

$$N(x) = \frac{(x - x_{min})}{(x_{max} - x_{min})}, \quad (2)$$

where *N(x)* is the normalized value, *x* is the initial value, and x_{min} and x_{max} are the minimum and maximum values in the original data, respectively.

To enhance the accuracy of satellite interferogram analysis and detect anomalous areas, such as vertical displacements or surface deformations, image processing methods based on linear filters in Python were applied. Decomposing complex filters into simpler components increases processing speed and efficiency (Sironi et al., 2015). Although the Canny and Sobel filters are mostly linear, integrating them with non-linear methods can further improve image quality by effectively reducing noise and preserving fine details. Combining linear and non-linear filtering methods allows for process optimization by addressing various noise types while preserving image structural integrity (Sironi et al., 2015). In this study, two main filtering methods were used for analyzing processed interferometric displacement maps: the Canny filter for edge detection and the Sobel filter for gradient calculation (Sonka et al., 2014). These methods allow the identification of key edges and details on interferograms in displacement maps for further analysis. The software code implementing these methods in Python is presented as a schematic (Fig. 3).

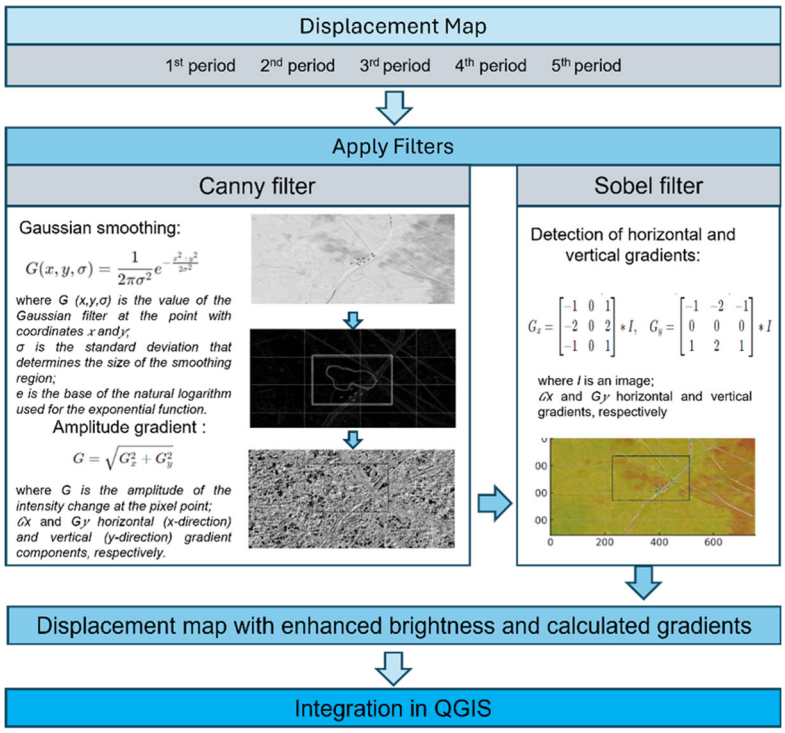

Fig. 3. Diagram of linear filter application for processed images

In the initial phase of the study, the displacement map generated in the SNAP software was loaded. For displacement map analysis, the image was converted to grayscale, allowing pixel intensity manipulation, as the focus is on brightness gradients representing deformations. Subsequently, the Canny filter, an effective method for edge detection based on pixel intensity gradient calculations, was applied. The Canny algorithm operates in several stages: first, the image is smoothed with a Gaussian filter to reduce noise. Then, intensity gradients are calculated at each point in the image. A double threshold selects potential edges by identifying points with strong gradients and those within the range between weak and strong thresholds (Zhang et al., 2019). The final stage involves suppressing continuity of weak edges not forming part of main edge lines. The result is a binary image where object edges are highlighted as bright lines.

Next, the Sobel filter is applied to calculate pixel intensity gradients in two mutually perpendicular directions: along the X and Y axes. Two different kernels are used to calculate derivatives in each direction. A kernel for the X direction computes changes in pixels horizontally, while a kernel for the Y direction captures vertical changes. The gradient magnitude at each point is computed as the vector sum of the gradients in the X and Y directions (Zhang et al., 2019). This method allows for detecting intensity changes that indicate contours and transitions between different elements in the image. The gradient magnitude reflects the sharpness of intensity variation, which can indicate deformations or other structural changes (Sironi et al., 2015).

The results obtained after applying both filtering methods are represented as images with highlighted contours (Fig. 4). For comparison, color scales and data normalization are used to ensure a consistent interpretation of displacement magnitude across different parts of the displacement map. This enables the identification of anomalous areas where changes in vertical surface displacements are observed.

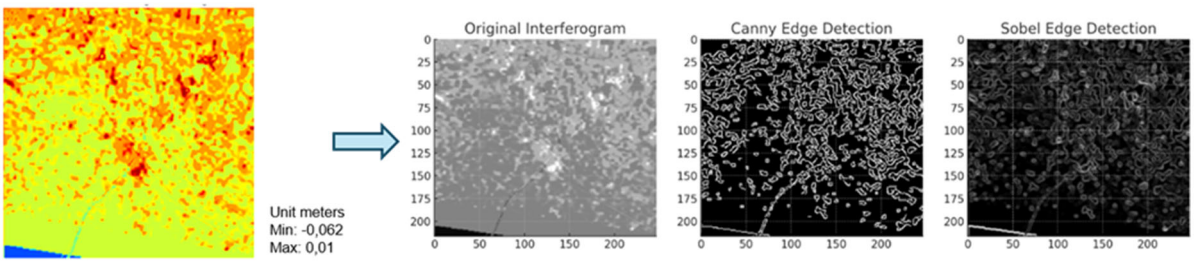

Fig. 4. Result of linear filter application for processed image during the 3rd period

To assess the degree of anomaly enhancement, the average values of contrast and sharpness are calculated for images before and after filter application. Contrast is defined as the difference between the mean pixel intensities of anomaly regions and the general background. An increase in this measure indicates better anomaly differentiation. Sharpness can be measured as the mean variability of gradients in the image; higher gradient levels after processing indicate improvement. Using pre- and post-processed images, pixel intensity values in anomaly and background areas are computed for each filter. The formula to determine the percentage of image improvement is presented as follows:

$$Result\ (\%) = \frac{(C_{before} - C_{after})}{C_{before}} \times 100\%, \qquad (3)$$

where C_{before} and C_{after} represent contrast or sharpness measures before and after processing, respectively.

After calculating data for both images (pre- and post-linear filter application), we obtain a percentage improvement. This quantifies how much clearer and more distinct the anomalies appear on the processed images. If improvement significantly exceeds 10–20 % (Schowengerdt, 2007; Gonzalez, & Wood, 2018), this suggests that the filters effectively highlight anomalies for further analysis. According to our research, improvement should be no less than 25 %. The difference between the original and filtered images, based on contrast, sharpness, and the number of detected edges, is computed in Python (Fig. 5).

Initially, both the original and filtered images, including filter results, are loaded into Python (see Fig. 5). For intensity gradient calculations, the Laplace operator is used to detect sharp pixel intensity transitions. The Laplacian effectively highlights areas of sharp intensity transitions, corresponding to edges or anomalies, aiding in quantitative evaluation of image sharpness and contrast (Gonzalez, & Wood, 2018). The percentage improvement for each pixel is calculated as the relative difference between the absolute gradient values of the processed and original images, allowing the assessment of local intensity changes. To avoid infinite values where the original gradient is zero, improvement at such pixels is set to zero. Then, the mean improvement across all pixels is calculated, providing an overall representation of texture changes after combined filtering. This mean value reflects the general intensity of changes between adjacent pixels, indicating edge enhancement quality. Following these procedures, the percentage improvement for each processed image is computed using formula (3), resulting in a 28 % improvement for the processed displacement maps. This figure indicates the effectiveness of the applied filters in highlighting specific characteristics, such as anomalies (vertical displacement values ∆h), which is essential for further data analysis.

The combination of these filters enables more precise information on displacement dynamics and the localization of deformation zones (Fig. 6), which is crucial for monitoring and identifying underground structure deformations.

This approach has allowed for the identification of areas with localized anomalous surface displacements that differ from the background values. Such zones may indicate potential deformations within the geotechnical environment. Values deviating from the average (background values of the area) may point to zones of potential subsidence or surface uplift, depending on the sign of the magnitude (Kril, & Orlenko, 2022).

The processed data was integrated into QGIS for further analysis and interpretation of potential risks of deformation of underground structures. The use of displacement calculations allowed visualizing the areas of subsidence and uplift of the surface of the study area, which contributed to a more accurate assessment of potential risks and possible future events. To highlight anomalous zones on the vertical displacement maps, we used a change in image gradation, which made it possible to identify areas with significant subsidence or uplift.

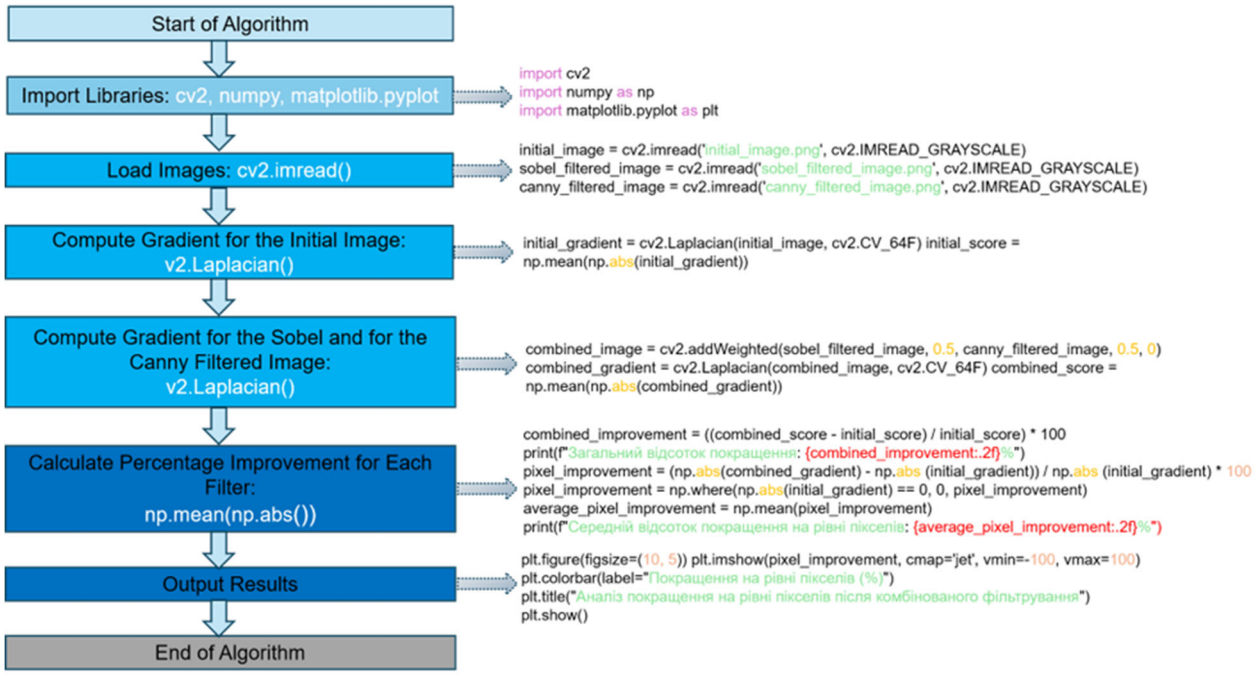

Fig. 5. The image comparison algorithm before and after filter application in Python environment

Visualization in QGIS was customized through the Symbols panel, where color gradations were used according to the displacement values. Rich and contrasting colors, such as red and blue, were used to clearly highlight anomalous areas, and setting thresholds for each category of displacement ensured that the display was sensitive, allowing even small changes to be identified (QGIS Documentation, n.d.). The Classification tool in QGIS helped to divide the data into different intervals, which made it easier to interpret the results and highlight specific areas that require special attention.

The contour analysis tool was used to automatically identify and outline the anomalous vertical displacement zones. Initially, the dataset containing the offset values was prepared as a raster layer. This format ensures high accuracy of spatial calculations and allows interpolation of contours based on numerical values (QGIS Documentation, n.d.). Then, using the Raster > Analysis > Contour menu in QGIS, the Contour tool was applied. The tool's parameters were configured in accordance with the specifics of the study, namely, the interval of isolines set the boundary values of displacements that delimited zones with different levels of risk. The resulting vector layer of contours was further stylized using color gradations and line thicknesses, which improved the visual delineation of subsidence or uplift risk zones. The classification of intervals in QGIS allowed us to detail the zones of abnormal changes, which made it possible to assess potential risks and possible future events in more detail.

Results

The assessment of vertical displacements was conducted over five periods within the defined study area, indicated by the black rectangle in Fig. 6c. Regions exhibiting anomalous zones, where the recorded Δh values significantly differ from the background levels within the study area, were identified. During periods 3–4, these anomalous zones are situated 75–160 m northwest of the tunnel within the study area, while in the southeastern section, they intersect the tunnel (Fig. 6a, b).

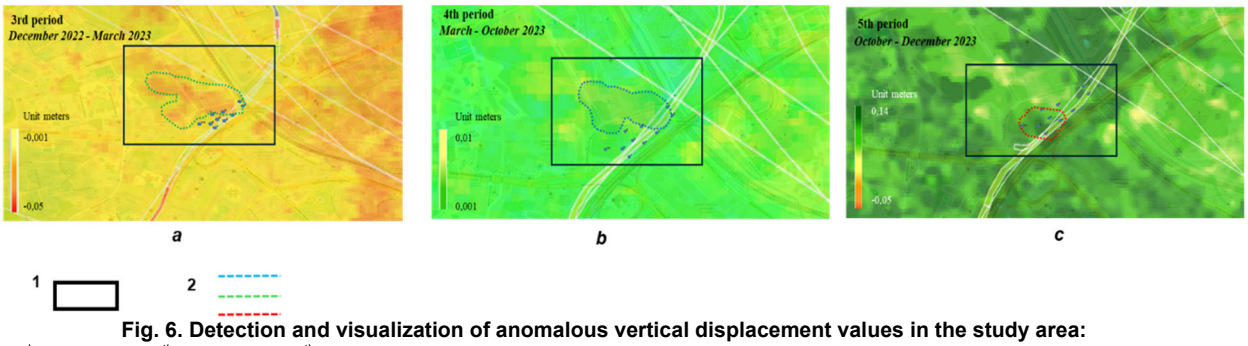

Fig. 6. Detection and visualization of anomalous vertical displacement values in the study area:
a) – 3rd period; b) – 4th period; c) – 5th period; 1 – the boundaries of the study area; 2 – contours of abnormal vertical displacements (Δh)

In the classified images for the fifth period, an anomalous zone appeared directly above the tunnel damage location (Fig. 6c). Over the three represented periods, the anomalous zones are observed to shift progressively toward the tunnel axis.

For displacement analysis, 10 control points were selected: four points directly above the metro tunnel (points 2, 3, 4, and 7), four points parallel to the tunnel, 35 meters to the left of the tunnel axis (points 1, 5, 6, and 8), and two points located 75 meters away (points 9 and 10). The vertical displacement values at these points for each observation period are presented in Tab. 2.

Table 2

The surface vertical displacements (m) for control points of the study area for different time periods

Point №	Observed time periods					Average value
	1st period	2nd period	3rd period	4th period	5th period	
	March – October 2022	October – December 2022	December 2022 – March 2023	March– October 2023	October– December 2023	
1	-0,09	-0,053	-0,034	0,085	0,116	0,0048
2	-0,078	-0,053	-0,041	0,051	0,108	-0,0026
3	-0,027	-0,03	-0,032	0,09	0,117	0,0236
4	-0,061	-0,057	-0,041	0,051	0,108	0
5	-0,09	-0,061	-0,039	0,064	0,11	-0,0032
6	-0,084	-0,036	-0,029	0,108	0,121	0,016
7	-0,088	-0,058	-0,018	0,142	0,133	0,0222
8	-0,088	-0,037	-0,019	0,138	0,132	0,0252
9	-0,069	-0,044	-0,039	0,057	0,109	0,0028
10	-0,072	-0,061	-0,046	0,04	0,102	-0,0074

The analysis of the obtained values reveals the following trends (Fig. 7). In the first study period (March–October 2022), the overall background Δh values are negative, ranging from -0.027 to -0.09. This indicates a phase with signs of surface subsidence or a downward trend. In the second period (October–December 2022), the negative values persist, but their absolute magnitude decreases, suggesting a slowing of subsidence dynamics and the beginning of stabilization (Δh → 0). Starting from the third period (December 2022–March 2023), a slight increase in values is observed, which continues into the fourth period (March–October 2023), where overall background values become exclusively positive. The fifth period (October–December 2023) solidifies these positive values, demonstrating stability following the previous increase. In this period, the identified anomalous zone coincides with the tunnel deformation and surface subsidence area, located near the 'Rozetka' store. Background Δh values are close to zero, indicating a leveling after the previous decline.

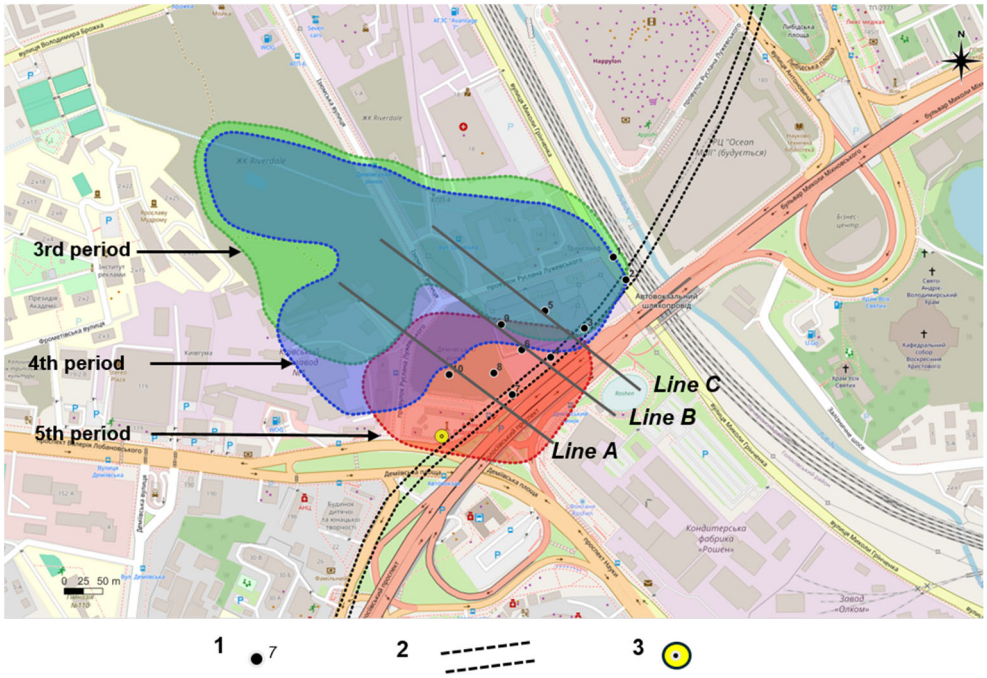

Fig. 7. Anomalous zones of vertical displacements within the study area across different time periods of observation:
1 – control points; 2 – subway tunnel; 3 – location of the 'Rozetka' store

The average vertical displacement at control points from March 2022 to December 2023 was 0.008 m. Average vertical displacements over five periods ranged from -0.03 m to 0.142 m. In 2022, a trend of surface subsidence was observed, with background values ranging from -0.061 m to -0.03 m. Absolute displacement values decreased from December 2022 to March 2023, with a mean absolute value of |0.0338| m.

In 2023, vertical displacements across the study area were generally positive (Fig. 8). Between March and October 2023 (4th period), positive surface displacements were recorded, with a maximum value of 0.142 m, which remained stable until December 2023, with a maximum recorded value of 0.133 m across ten control points. This may indicate changes in stress within the geotechnical environment in the study area.

The comparison of displacements at control points along lines over the metro tunnel (Line B, see Fig. 7) showed that, despite overall positive displacements, values directly above the tunnel were 0.035 m lower than those at a distance of 35 meters and 0.0145 m lower than those at 75 meters. This indicates that the surface directly above the tunnel undergoes more significant subsidence than areas located 100 m away, leading to the formation of subsidence zones (Fig. 8).

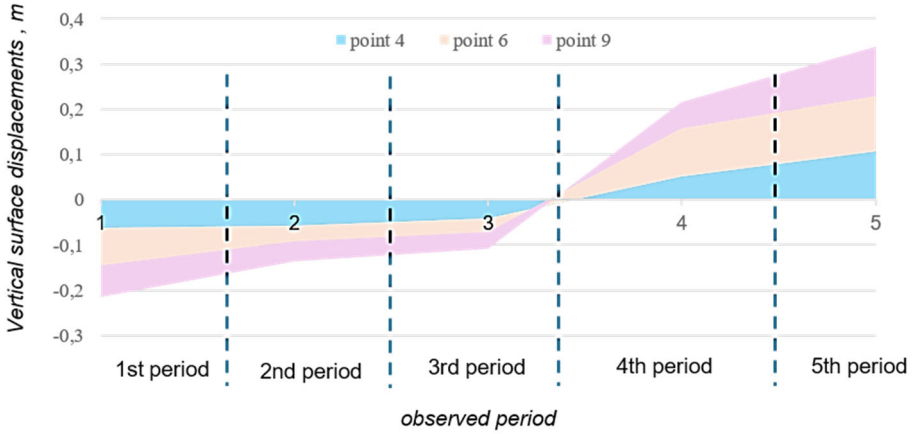

Fig. 8. Vertical displacements at control points 4. 6. 9 along line B

Discussion and conclusions

Using the section of the tunnel between the Demiivska and Lybidska stations as a case study, this research demonstrates the feasibility of employing vertical surface displacement analysis from remote sensing data as an indicator of deformation in underground infrastructure. Data processing utilized D-InSAR methods in combination with linear filters.

Interpretation was conducted with linear filtering and normalization techniques, allowing the visualization and comparison of images on a unified color scale and consistent gradient for vertical displacements. The combination of linear filtering methods optimized processing by addressing noise types such as geometric distortions, shadowing, and multipath noise, while maintaining the structural integrity of the image. Our findings indicate that for significant results, an improvement rate of at least 25 % is required. Applying linear filters to the study images achieved a 28 % enhancement in contrast and sharpness, demonstrating the effectiveness of these methods for anomaly detection in subsequent analysis. The results underscore the importance of quantitative assessment of clarity and contrast for more precise identification of specific features in processed data, particularly in complex, noisy, or low-contrast images of urbanized areas.

Despite the significant image quality improvement provided by these methods, challenges remain in balancing noise reduction with the preservation of critical image details, highlighting the need for ongoing research in this area.

Throughout the observation periods, anomalous zones were observed to shift toward the tunnel axis. During the last period, the anomalous zone coincided with the deformation site of the tunnel and surface subsidence (near the 'Rozetka' store). Observations from March 2022 to December 2023 indicated both positive and negative displacements across the study area: negative displacements were observed in periods 1–3 (2022) and positive displacements in periods 4–5 (2023). In each period, control points directly above the tunnel (points 2, 3, 4, and 7) exhibited anomalous values compared to background levels across the study area.

This research establishes a foundation for the further development of methodological approaches to analyzing potential deformations in underground structures based on indicative features of surface dynamics–specifically, vertical displacements. Its practical application is crucial for monitoring the status of Kyiv Metro lines, particularly shallow-depth lines like the Obolonsko-Teremkivska line, and for preventing similar incidents in the future.

The research was conducted within the framework of the scientific theme III-5-23, "Engineering and Geological Foundations for Urban Development and the Strategic Mastery of Underground Space," state registration number is 0123U100129.

Authors' contribution: Vasyl Hudak – writing (review and editing), methodology; Tetyana Kril – conceptualization, data validation, methodology, writing (original draft); Vitalii Zatserkovnyi – formal analysis.

References

Caduff, R., Schlunegger, F., Kos, A., & Wiesmann, A. (2015). A review of terrestrial radar interferometry for measuring surface change in the geosciences. *Earth Surface Processes and Landforms*, 40(2), 208–228. https://doi.org/10.1002/esp.3656

Ferretti, A., Prati, C., & Rocca, F. (2000). Nonlinear subsidence rate estimation using permanent scatterers in differential SAR interferometry. *IEEE Transactions on Geoscience and Remote Sensing*, 38(5), 2202–2212. https://doi.org/10.1109/36.868878

Forsyth, D. A., & Ponce, J. (2012). *Computer vision: A modern approach* (2nd ed.). Pearson.

Gabriel, A. K., Goldstein, R. M., & Zebker, H. A. (1989). Mapping small elevation changes over large areas: Differential radar interferometry. *Journal of Geophysical Research: Solid Earth*, 94(B7), 9183–9191. https://doi.org/10.1029/JB094iB07p09183

Gonzalez, R. C., & Woods, R. E. (2018). *Digital image processing* (4th ed.). Pearson. https://dl.icdst.org/pdfs/files4/01c56e081202b62bd7d3b4f8545775fb.pdf

Iglesias, R., Mallorqui, J. J., Monells, D., López-Martínez, C., Fabregas, X., Aguasca, A., & Corominas, J. (2015). PSI deformation map retrieval by means of temporal sublook coherence on reduced sets of SAR images. *Remote Sensing*, 7(1), 530–563. https://doi.org/10.3390/rs70100530

Italian National Research Council. (2017). A review of interferometric synthetic aperture RADAR (InSAR) multi-track approaches for the retrieval of Earth's surface displacements. *Applied Sciences*, 7(12), 1264. https://doi.org/10.3390/app7121264

Kril, T. (2017). Causes of some hazardous engineering geological processes on urban territories. *3rd International Conference on Applied Geophysics E3S Web of Conferences*, 24, Article 01009. https://doi.org/10.1051/e3sconf/20172401009

Kril, T., & Orlenko, T. (2022). Surface Dynamics Assessment as a Landslide Hazard Factor by Remote Sensing Data. *16th International Conference Monitoring of Geological Processes and Ecological Condition of the Environment*, 2022, 1–5. https://doi.org/10.3997/2214-4609.2022580246

Kyiv City Council. (2023, December 8). Train services between the metro stations 'Demiyivska' and 'Teremky' will be closed from December 9 for urgent repair of the transit tunnel. *Kyiv City Portal*. https://kyivcity.gov.ua/news/rukh_pozdiv_mizh_stantsiyami_metro_demivska_ta_teremki_zakriyut_iz_9_grudnya_dlya_terminovogo_provedennya_remontu_peregrinnogo_tunelyu/

Minh, D. H. T., Hanssen, R., & Rocca, F. (2020). Radar interferometry: 20 years of development in time series techniques and future perspectives. *Remote Sensing*, 12(9), 1364. https://doi.org/10.3390/rs12091364

Ministry of Regional Development of Ukraine. (2018). *Content and structure of the zoning plan. DBN B.1.-22:2017* (effective from 2017-12-27). (State Building Codes of Ukraine).

Nguyen, C. G., Dang, V. K., & Vu, A. T. (2020). Monitoring land subsidence evolution in the central urban region of Hanoi City, Vietnam. *International Journal of Civil Engineering and Technology*, 11(6), 18–30. https://doi.org/10.34218/IJCIET.11.6.2020.003

Orlenko, T. A. (2024). *Remote geoecological monitoring technique for landslide processes: An example of the right bank of the Kaniv Reservoir* [Doctoral dissertation, State Institution "Scientific Center for Aerospace Research of the Earth, Institute of Geological Sciences, National Academy of Sciences of Ukraine"]. https://www.casre.kiev.ua/images/files/phd/orlenko/FINAL_Diss_Orlenko.pdf

Pawluszek-Filipiak, K., Ilieva, M., Wielgocka, N., & Stasch, K. (2022). Evaluation of synthetic aperture radar interferometric techniques for monitoring of fast deformation caused by underground mining exploitation. https://doi.org/10.4995/JISDM2022.2022.13863

Piestova, I., Dugin, S., Orlenko, T., & Svideniuk, M. (2020). Assessing and forecasting landslide hazards of The Right Bank of the Kanev reservoir based on radar remote sensing data with corner reflectors using. *XIV International Scientific Conference "Monitoring of Geological Processes and Ecological Condition of the Environment"*, 1, 1–5. https://doi.org/10.3997/2214-4609.202056082

QGIS Documentation. (n.d.). Creating contours and using interpolation in QGIS. *QGIS Training Manual*. Retrieved November 10, 2024, from https://docs.qgis.org/latest/en/docs/training_manual/processing/interp_contour.html

Schowengerdt, R. A. (2007). *Remote sensing: Models and methods for image processing* (3rd ed.). Academic Press.

Serco Italia SPA. (2018). *Land Subsidence with Sentinel-1 using SNAP* (Version 1.2). Retrieved from RUS Lectures at https://rus-copernicus.eu/portal/the-rus-library/learn-by-yourself/

Sironi, A., Tekin, B., Rigamonti, R., Lepetit, V., & Fua, P. (2015). Learning Separable Filters. *IEEE Transactions on Pattern Analysis and Machine Intelligence*, 37(1), 94–106. https://doi.org/10.1109/TPAMI.2014.2343229

Sonka, M., Hlavac, V., & Boyle, R. (2014). *Image Processing, Analysis, and Machine Vision*. Cengage Learning.

Zhang, L., Li, X., & Yang, J. (2019). Recent advances in edge detection: A review. *IEEE Access*, 7, 76774–76793. https://doi.org/10.1016/j.neucom.2022.06.083

Отримано редакцією журналу / Received: 26.12.24
Прорецензовано / Revised: 24.01.25
Схвалено до друку / Accepted: 12.03.25

Василь ГУДАК, асп.
ORCID ID: 0009-0002-7333-0409
e-mail: gudak_vasyl@knu.ua
Київський національний університет імені Тараса Шевченка, Київ, Україна

Тетяна КРІЛЬ, канд. геол. наук,
ORCID ID: 0000-0002-4324-9231
e-mail: kotkotmag@gmail.com
Інститут геологічних наук, Національна академія наук України, Київ, Україна

Віталій ЗАЦЕРКОВНИЙ, д-р техн. наук, проф.
ORCID ID: 0009-0003-5187-6125
e-mail: vitalii.zatserkovnyi@knu.ua
Київський національний університет імені Тараса Шевченка, Київ, Україна

ДИСТАНЦІЙНИЙ МОНІТОРИНГ ВЕРТИКАЛЬНИХ ЗМІЩЕНЬ ЗЕМНОЇ ПОВЕРХНІ ЯК ІНДИКАТОРІВ ДЕФОРМАЦІЇ ПІДЗЕМНИХ СПОРУД

В с т у п . ***Присвячено аналізу вертикальних зміщень за даними дистанційного зондування як ідентифікатора небезпечних інженерно-геологічних процесів на ділянках із підземною інфраструктурою. Дослідження проведено на прикладі ділянки перегінного тунелю між станціями "Деміївська" і "Либідська" Київського метрополітену. У грудні 2023 р. виявлено нерівномірні процеси розущільнення, віброповзучості ґрунтового масиву навколо тунельної оправи та з'явився ризик втрати стійкості тунельних споруд і виникнення аварійної ситуації.***

М е т о д и . ***У досліджені застосовано метод диференціальної інтерферометрії D-InSAR, що використовується для моніторингу деформацій земної поверхні через аналіз фазових змін між радіолокаційними зображеннями. Для прибирання шумів на опрацьованих зображеннях через часову та геометричну декореляцію, атмосферні збурення і шумові перешкоди використано низку корекційних процедур. Для підвищення точності значень застосовано корекційні та фільтраційні методи, а саме лінійні фільтри Кенні та Собеля. Їх застосування до опрацьованих космічних знімків дало змогу підсилити контури зафіксованих вертикальних зміщень та зменшити шум геометричних спотворень, зберігаючи структурну цілісність зображень. За нашими розрахунками для ефективного виявлення аномалій на знімках урбанізованих територій потрібен мінімальний поріг у 25 % контрастності та чіткості зображення. Використання фільтрів для підкреслення інтенсивних змін дало змогу досягти 28 % підвищення чіткості, що свідчить про високу ефективність обробки для подальшого аналізу карт зміщень та інших параметрів, пов'язаних із вертикальними зміщеннями.***

Р е з у л ь т а т и . ***За вертикальними зміщеннями на досліджуваній території встановлено аномальні зони. За спостережний період 2022–2023 рр. зафіксовано їх переміщення у напрямку до осі тунелю метро. Вертикальні зміщення безпосередньо над місцем провалів поряд із магазином "Розетка" виявлено у п'ятий спостережуваний період – жовтень–грудень 2023 – час закриття тунелю на ремонтні роботи. Загалом значення зміщень з від'ємних у 2022 р. змінилися на додатні в 2023 р., що вказує на те, що зміщення могли стати одним з індикаторів активізації деформацій підземної споруди. Використання фільтрів дало змогу отримати точнішу інформацію про динаміку переміщень та локалізацію зон деформації протягом періодів спостереження. В останньому періоді аномальна зона збіглася з місцем деформацій тунелю та осідання поверхні.***

В и с н о в к и . ***На прикладі ділянки перегінного тунелю показано можливість використання аналізу вертикальних зміщень поверхні, проведеного методом D-InSAR разом з комбінацією фільтрів Кенні та Собеля для відстеження вертикальних зміщень поверхні, що є важливим для моніторингу стану підземних об'єктів та упередження можливих аварій. Це дослідження закладає основу для подальшого розвитку методологічних підходів до аналізу потенційних деформацій підземних конструкцій на основі динаміки поверхні (вертикальних зміщень). Подальше вдосконалення методології сприятиме забезпеченню точності і надійності даних у контексті моніторингу підземних конструкцій.***

К л ю ч о в і с л о в а : ***вертикальні зміщення земної поверхні, супутникові знімки, D-InSAR, підземні споруди, аварія на станції метро "Деміївська".***

Автори заявляють про відсутність конфлікту інтересів. Спонсори не брали участі в розробленні дослідження; у зборі, аналізі чи інтерпретації даних; у написанні рукопису; в рішенні про публікацію результатів.

The authors declare no conflicts of interest. The funders had no role in the design of the study; in the collection, analyses, or interpretation of data; in the writing of the manuscript; or in the decision to publish the results.